DETECTION OF BATTLEFIELD VISIBILITY FROM SATELLITE

Kenneth R. Knapp, Kenneth Eis, Thomas Vonder Haar and Kirk Fuller
Colorado State University / Cooperative Institute for Research in the Atmosphere
Fort Collins, CO 80523
knapp@CIRA.colostate.edu

Abstract

Today's smart weapons rely to a large extent on infrared and visible sensors seeing their targets. Atmospheric aerosols, including smoke, dust, and pollutants, contribute to the degradation of the performance of these weapons. Atmospheric scattering, due to aerosols, limits the lock-on range of most smart weapons today. CIRA is working on determining horizontal visibility and aerosol parameters remotely from the Next Generation Geostationary Observational Environmental Satellite (GOES-8) using a doubling and adding radiative transfer model developed at Colorado State University. The model has been previously used to investigate optical depth and transport of the Kuwaiti Smoke Plumes after the Persian Gulf War. Model output is validated using the National Park Services Interagency Monitoring of Protected Visual Environment (IMPROVE) data set.

1. Introduction

Aerosols degrade the performance of visible and infrared sensors, so it is important to know the extent of aerosols at and around a target. These aerosols scatter radiation emitted from or reflected by the target (signal) away from the sensor, and scatter ambient radiation (noise) into the sensor's field of view (FOV). Satellites can provide an estimation of the extinction characteristics of aerosols. Aerosols scatter solar radiation reflected by the ground (satellite noise) out of the satellite FOV and ambient solar radiation into the sensor FOV (signal). In retrieving optical depths, the noise of aerosols in satellite imagery becomes signal. For most aerosols, this has a brightening effect over dark surfaces (ocean or dense vegetation) and a darkening effect over bright surfaces. This change in the amount of solar radiation received at the satellite is dependent upon the amount of aerosol in the atmosphere, the absorptive and directional scattering characteristics of the aerosol, as well as the scattering angle from the sun to the aerosol back to the satellite (sun-earth-satellite geometry).

Previous work has concentrated on retrieving aerosol optical depth using polar orbiting satellites, such as Landsat or NOAA instruments, which have poor temporal coverage. The GOES-8 satellite provides better imagery than its predecessor GOES-7 at higher temporal resolution than the polar orbiting sensors. Work was concentrated on sensing aerosols over IMPROVE sites in the Eastern U.S. An existing Adding/Doubling Radiative transfer model (Greenwald and Stephens, 1988) was used to retrieve optical depths from GOES-8 visible imagery with assumed aerosol optical properties. Although, recent work has allowed estimation of these aerosol optical properties from *in situ* chemical composition data measured by the IMPROVE network. Comparisons of the model output were made to measurements from nephelometers and transmissometers also of the IMPROVE network. Retrievals were for 4 case periods (9 days each) during the summer of 1995 over the Eastern U.S. An error budget was

calculated and retrievals had an estimated error of $\Delta\tau = \pm(0.05 - 0.16)$ for τ ranging from 0.1 to 1.0.

Section 2 presents the retrieval method followed by a description of the datasets and the Adding/Doubling model in sections 3 and 4. Comparisons to surface data are shown in section 5, and conclusions are made in section 6

2. Optical Depth Retrieval Method

Optical depths were retrieved from GOES-8 imagery using an Adding/Doubling radiative transfer (A/D) model. Figure 1 shows a schematic of the retrieval process. The A/D model uses reflectance measured by the GOES-8 visible channel and assumed aerosol optical properties as input. Data from the GOES-8 system includes a background reflectance for a particular pixel, the reflectance of a haze over the same pixel and sun-earth-satellite geometry. The background reflectance was chosen as the lowest (darkest) pixel value during a ten day period for that specific time, excluding cloud shadows. The aerosol optical properties used in the A/D model are asymmetry parameter (g) and the single scatter albedo (ω_o). The A/D model calculates optical depth as the amount of aerosol with the assumed optical properties needed to increase the satellite detected reflectance from the background reflectance to that observed by the satellite with haze present. This method of retrieval requires excellent pixel co-registration and accurate sensor calibration. Co-registration is the controlling of the sensor such that the same pixel represents the same earth point in successive images and noise is estimated at ± 7 pixels between successive days (Menzel and Purdom, 1994). However, imagery used in this study was manually navigated using visible surface features (e.g. lakes and rivers) to an estimated ± 1 pixel. Calibration of the GOES-8 data is the conversion of transmitted GOES-8 counts to a reflectance value. This was accomplished using calibration coefficients from the home page of Dennis Chesters at NASA/GSFC. These were pre-flight calibration values which do not account for possible in-flight sensor degradation.

Optical depths were retrieved over the Eastern U.S. for four 9-day periods during the summer of 1995 over IMPROVE sites. These periods, which occurred in late May, mid July, mid August and late August, were determined from IMPROVE data and daily weather maps. IMPROVE data showed high extinction and scattering coefficients and surface analyses showed high pressure areas over the east during these times.

3. Data

The GOES-8 satellite has many advantages over its predecessor, GOES-7, for aerosol optical depth retrieval. GOES-7 had a non-linear 6-bit digitization, whereas GOES-8 has a linear 10-bit digitization, which allowed for more resolved changes in satellite detected radiance. The signal-to-noise ratio was improved by a factor of 4, providing higher confidence of the pixel count. This high quality sensor at geostationary orbit provides visible imagery at 15 minute intervals over the continental U.S.

A large, Eastern U.S. sector of GOES-8 imagery was archived during the summer of 1995 for morning hours, 12:15 through 15:31 z for the purpose of retrieving τ. The sector area was determined by positions of IMPROVE sites. It was later expanded west in July to incorporate another IMPROVE site (the nephelometer at Mammoth Caves National Park) and extended until 20:45z, to include more daylight hours for comparison.

The IMPROVE network consists of more than 60 aerosol monitoring sites at National Parks (FJ.P.) around the United States. Instruments used to monitor the air quality include: transmissometers, nephelometers, aerosol collection instruments and atmospheric state variable instruments.

There are three nephelometer sites which measure the surface scattering coefficient (b_{scat}) in the area encompassed by the GOES-8 collection region at: Dolly Sods, West Virginia near the Monongehela National Forest (DOSO), Great Smoky Mountains N. P., Tennessee (GRSM), and Mammoth Cave N. P., Kentucky (MACA). The nephelometer measures atmospheric scattering at the wavelength 0.55 pm. Also, Shenandoah N.P. in Virginia (SHEN) has a transmissometer that measures the extinction coefficient (b_{ext}) at 0.55pm. Measurements by these instruments will be referred to as optical coefficients, because they refer to two separate types of measurements. They are used nearly synonymously here because the absorption coefficient is usually negligible.

Also, temporal, spatial and spectral differences in these datasets increase error in comparing their measurements of aerosols to retrieved optical depths. GOES-8 imagery is available over the Eastern U.S. at 15 minute intervals, whereas the IMPROVE data reports conditions on the hour. Retrievals of optical depth from GOES-8 were averaged to the nearest hour when compared to surface data. Also, the IMPROVE instruments have a sample volume which is about 10 orders of magnitude smaller than the GOES-8 visible channel sample volume, which is a vertical cone through the atmosphere with a 1 km^2 footprint. And spectrally, the GOES-8 visible channel has a range of 0.55-0.75μm, while the IMPROVE instruments have a narrow detection band centered at 0.55 μm.

4. **Adding/Doubling Model**

The adding/doubling, multiple scattering model used in this study was developed by Greenwald and Stephens (1988). It was designed to perform sky color, intensity and object contrast simulations (Tsay et. al., 1991). After some modifications by Graeme Stephens and Jan Behunek, it currently calculates optical depth from satellite detected reflectance, sun-earth-satellite geometry, and aerosol optical properties. The following is an overview of the model and its application to aerosol optical depth retrieval. For a more rigorous description of model derivation, see Greenwald and Stephens (1988). This method has previously been used to retrieve optical depths from smoke plumes during the 1991 Kuwaiti oil fires (Behunek et al., 1993).

Theory

The equation of radiative transfer for a plane-parallel, scattering atmosphere is

$$\mu \frac{dL(\tau;\mu,\phi)}{d\tau} = -L(\tau;\mu,\phi) + \frac{\omega_o}{4\pi}\int_0^{2\pi}\int_{-1}^{1} P(\tau;\mu,\phi,\mu',\phi')L(\tau;\mu',\phi')d\mu' d\phi' + J(\tau;\mu,\phi) \qquad (1)$$

where J, the "pseudo-source" term, is

$$J(\tau;\mu,\phi) = \frac{\omega_o}{4\pi}F_o P(\tau;\mu,\phi,-\mu_o,\phi_o)e^{-\tau/\mu_o} + \frac{\omega_o}{4\pi}F_o\rho_s P(\tau;\mu,\phi,\mu_o,\phi_o)e^{-(2\tau^*-\tau)/\mu_o} \qquad (2)$$

L is radiance, $\mu=\cos\theta$, θ and ϕ are geometric angles, τ is optical depth, P is the phase fiction, F_o is the solar irradiance at the top of the atmosphere (TOA), ρ_s is the surface specular reflectance

and τ^* is the optical depth of the atmosphere. The first term in equation 1 and the second term in equation 2 represent the extinction of the solar radiance reflected by the surface or aerosol. The second term in equation 1 and the first term in equation 2 represent the radiance scattered by the aerosol into the satellite FOV. The scattering of reflected radiance from a nearby pixel into the satellite FOV (a blurring effect) is not accounted for by this model. J is a pseudo-source term because there is no source for visible radiation in the atmosphere, but the aerosol scattering of the direct solar beam can act as a source. The phase function used is the Henyey-Greenstein phase function.

By expanding the phase function using Legendre polynomials, the intensity using Fourier series and using a Gaussian quadrature approximation, equation 1 is transformed into a series of matrix equations that can be solved using the adding/doubling technique. The end product is a 32-stream radiative transfer model which calculates the theoretical satellite observed reflectance (ρ_{sat}), at 16 satellite zenith angles@) due to an aerosol layer with the optical parameters g and ω_o at the sun-earth-satellite geometry (p_o, ϕ_o, ϕ) and ρ_s determined from GOES-8 imagery.

Optical depth was then retrieved iteratively. By using the known latitude, longitude and time of the image, the scattering angles (p, ϕ, μ_o, ϕ_o) were calculated. A background reflectance was found through an algorithm that used the darkest pixel over a time series of images. Then assuming some g and ω_o and starting with an initial guess for τ, a theoretical satellite-detected reflectance was calculated. This was then compared to the observed satellite reflectance, and a new estimate of τ was calculated from the difference in reflectance, iteratively solving for $\tau_{A/D}$.

Because the model used a background reflectance as a comparison to reflectance of haze, it only calculated the difference in τ between the background reflectance and haze satellite images due to an increase in τ from a layer of aerosols with the assumed optical properties. The reflectance used is not the actual surface reflectance, rather the darkest pixel at a location measured during the case, a background reflectance. This contained some background aerosol signal. Because the optical depth is a difference, the nearly constant Rayleigh component and background aerosol optical depth are subtracted out. So, ρ_s is a background reflectance, not a surface reflectance.

Critical Albedo

Investigation of model output has shown a scenario that renders optical depth undetectable. The same aerosol that brightens an originally dark image (e.g. a dense forest) would also darken an originally bright image (e.g. snow cover). Between these effects is a surface reflectance for which changes in aerosol amount have no effect on the reflected radiance. This condition is called the critical albedo region. It is defined as a range of surface reflectance where an increase in aerosol optical depth has no detectable effect in the amount of reflected solar radiation. This critical albedo is a function of the optical parameters of the aerosol and the solar geometry. Figure 2 shows an example of this effect. The dashed lines represent the change in satellite-detected reflectance due to an optical depth as a function of surface reflectance calculated from the A/D model. The scatter of dots are actual points from a GOES-8 visible image of the Shenandoah area. These lines cross at ρ_s = 0.3, showing that for the assumed aerosol optical properties the background reflectance do not approach the critical albedo region, which is 0.3 for this case.

Model Sensitivity and Error

Errors such as co-registration and calibration have already been discussed. Errors in the retrieval due to uncertainty in the AID model parameters also exist. Table 1 shows the percent change in $\tau_{A/D}$ due to a 5°/0 change in an input parameter. It is clear that errors in the surface reflectance or single scatter albedo can cause large errors in the retrieval of optical depth. Uncertainty in the surface reflectance was minimized in the data processing. Aerosol optical parameters used here (ω_o = 0.956 and g = 0.75) were chosen from previous work in the Eastern U.S. and have an estimated error of ± 3 and 1 % for g and ω_o respectively. Therefore, $\tau_{A/D}$ retrievals have an estimated error of $\Delta\tau$ = +(0.05-0.16) for $\tau_{A/D}$ values of 0.05 to 1.0.

5. **Comparison to Surface Data**

Directly comparing surface terms (b_{ext} or b_{scat}) to a vertically integrated quantity (τ) can be ambiguous. These coefficients vary with height and are related to τ by:

$$\tau = \int_{sfc}^{TOA} b_{ext}(z)dz = \int_{sfc}^{TOA} \left[b_{scat}(z) + b_{abs}(z)\right]dz \approx \int_{sfc}^{TOA} b_{scat}(z)dz \qquad (3)$$

where $b_{abs}(z)$ is the absorption coefficient of the aerosol as a function of height in the atmosphere. The last relation in equation 3 is justified when absorption is small. Because the background reflectance is used, the change in optical depth between the pristine day and the hazy day is detected. This change in optical depth is assumed to be confined to a well mixed boundary layer. Then the optical coefficients are no longer a function of height, thus:

$$\tau = b_{ext}\,\Delta z \approx b_{scat}\,\Delta z \qquad (4)$$

where the optical coefficients are vertical averages in a boundary layer with height Az.

b vs. $\tau_{A/D}$

Figure 3 shows scatter plots of satellite retrieved optical depth vs. optical coefficients from IMPROVE data (b_{ext} and b_{scat}) for each case and site. The correlation coefficients of the graphs are provided in Table 2. Overall, 10 of 13 show positive correlation, with better comparisons at GRSM. When first approaching these comparisons, it was expected that under low haze conditions (small b), there would be more noise because of less aerosol signal. Conversely, we expected more accuracy under hazy conditions. This can be seen in the plots for MACA cases 2 and 4 for $b < 0.3\,km^{-1}$, although not all plots show this trend. Plots for case 1 have a small range of b values, which provide little insight into the retrieval accuracy. Cases 3 and 4 (late summer) seemed to have better correlations and more data points than earlier cases. Also, only three cases had any values of $b > 0.6$ km-l (visibility less than 6 km). Other comparisons (e.g. DO SO case 2 and MACA case 3) show broad distribution of points without a definite relationship. This could be due to many reasons such as variations in aerosol vertical structure, aerosol optical properties or cloud contamination.

These plots are dependent upon the vertical distribution of the aerosol. An attempt to account for the variation in Az was made using National Weather Service rawinsonde data, but variations in terrain and the large spacing between stations did not increase the correlation of the comparisons. A Lidar needs to be co-located with the surface aerosol observations, because current understanding of the vertical distribution of aerosols is limited. The broad distribution of points could also occur from a layer of aerosols advected above the boundary layer. Clouds were

visually filtered prior to optical depth retrievals. Errant τ retrieval over clouds (especially thin cirrus) would return erroneously high τ values. Changes in surface reflectance properties due to rain might also affect the retrievals. For instance, the ranges of optical coefficients in case 1 were limited due to rain occurrences twice during the time period. Other cases had no rain or rain near the end or beginning of the case. In summary, encouraging comparisons were found over GRSM and during the late summer cases.

IMPROVE Visibility vs. Satellite Visibility

Converting these values to a visibility requires use of the Koschmeider equation:

$$\mathrm{Vis} = \frac{3.912}{b_{ext}}. \tag{5}$$

The retrieved optical depth can be converted to b_{ext} using an estimate of Az in equation 4. This has been done for GRSM case 2 (not shown in figure 3). Figure 4a shows the comparison of $\tau_{A/D}$ vs. b_{scat}. Figure 4b shows the same comparison in visibility coordinates ($\tau_{A/D}$ was converted using Az = 1.5km). It can be seen that there is less noise for lower risibilities (Vis < 25 km), but the lowest visibility measured by the IMPROVE site is greater than 10 km. The region of risibilities less than 10 km would provide adequate aerosol signal, but no comparisons have more than one value that low.

6. Conclusions and Future Work

Aerosol optical depths were retrieved over IMPROVE sites in the Eastern U.S. with encouraging results. Correlations of most comparisons were positive and statistically significant. Although uncertainties exist that cause scatter in the comparisons. Aerosol vertical structure variations, relative humidity changes (which causes changes in g and ω_o), cloud contamination and changes in surface reflectance features (e.g. due to rain events) are speculated causes in some of the less correlated comparisons. Knapp (1996) showed that by adjusting g and ω_o using an a priori surface relative humidity increased correlation in the comparisons. Future retrievals should include estimation of boundary layer moisture content. More comparisons need to be made in heavy haze conditions, to further define what the lower limit of aerosol detectability is. Also, future work needs to have continuous optical depth retrievals, rather than case studies as presented here. This would allow insight into the temporal variability of the surface reflectance and the affect rain has on the retrievals. IMPROVE sites in this work were located in densely forested areas. Further work should also include areas with different background reflectance (deserts, plains, etc.).

Using this remote sensing method, aerosol climatologies could be developed globally that would allow DOD mission planners to get a first guess on the operational limits of their standoff weapons' performance,

Acknowledgments

The funding for this work was made possible through the Department of Defense Center for Geosciences - Phase II, grant #DAAH04-94-G-0420.

References

Behunek, J.L, J.M. Forsythe, and T.H. Vender Haar, 1993: Satellite analysis of Kuwaiti oil smoke plumes. In Proceedings of the 1993 Battlefield Atmospherics Conference, 30 Nov. -2 Dec. 1993, Las Cruces, NM, U.S. Army Research Lab., White Sands Missile Range, NM, 357-368.

Chesters, Dennis, 1994: http://climate-f.gsfc.nasa.gov/~chesters/text/imager.calibration.html

Greenwald, T. J. and G. L. Stephens, 1988: Application of an Adding-Doubling Model to Visibility Problems, C.S.U. Atm. Sci. Paper, 89 pp.

Kaufman, Y. J., 1987: Satellite Sensing of Aerosol Absorption, J. *Geophys. Res.*, 92, 4307-4317.

Knapp, Kenneth R., 1996: Radiative effects of boundary layer aerosols: Detectability by GOES-8 and estimation of their direct effect, Master's of Science Thesis, C. S. U., 112 pp.

Menzel, W. P. and J. F. W. Purdom, 1994: Introducing GOES-I: The first of a new generation of Geostationary Operational Environmental Satellites, *Bull. of the Amer. Met. Sot., 75, 757-781.*

Tsay, S.-C., G. L. Stephens and T. J. Greenwald, 1991: An investigation of aerosol microstructure on visual air quality, *Atm. Env, 25A,* 1039-1053.

Table 1- The percentage change in τ due to a 5% change in the input parameter.

INPUT PARAMETER	% CHANGE IN τ
Calibration	10
Asymmetry	20
Surface Reflectance	34
Single Scatter Albedo	35

Table 2- Table of correlation coefficients (and number of samples) for all cases and IMPROVE sites comparing b vs. τ_{Am}.

	CASE 1	CASE 2	CASE 3	CASE 4
	May 20-28	July 10-19	Aug. 8-18	Aug. 28- Sep. 6
DOSO	0.224 (10)	-0.390 (20)	-	0.701 (21)
GRSM	0.870 (16)	0.763 (30)	0.719 (21)	0.438 (41)
MACA	-	0.265 (39)	0.562 (29)	0.536 (53)
SHEN	0.993 (9)	0.669 (9)	-	0.813 (20)

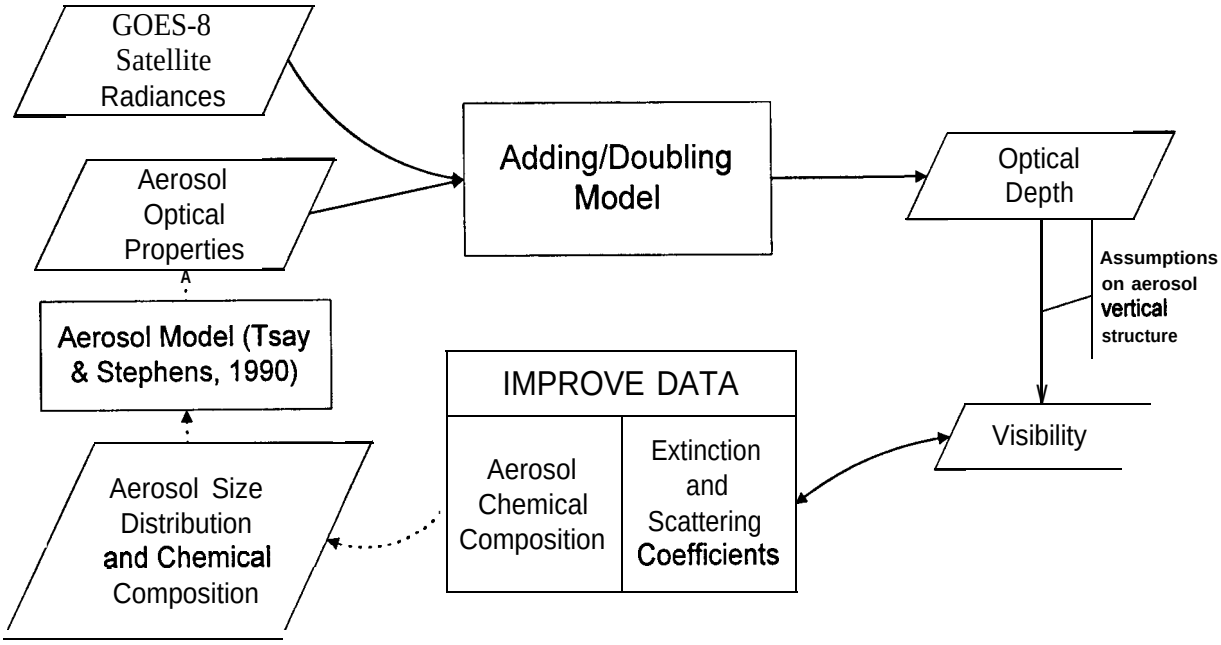

Figure 1- Retrieval method flowchart. Solid arrows depict steps used in current results. Dashed arrows represent steps now possible through recent work.

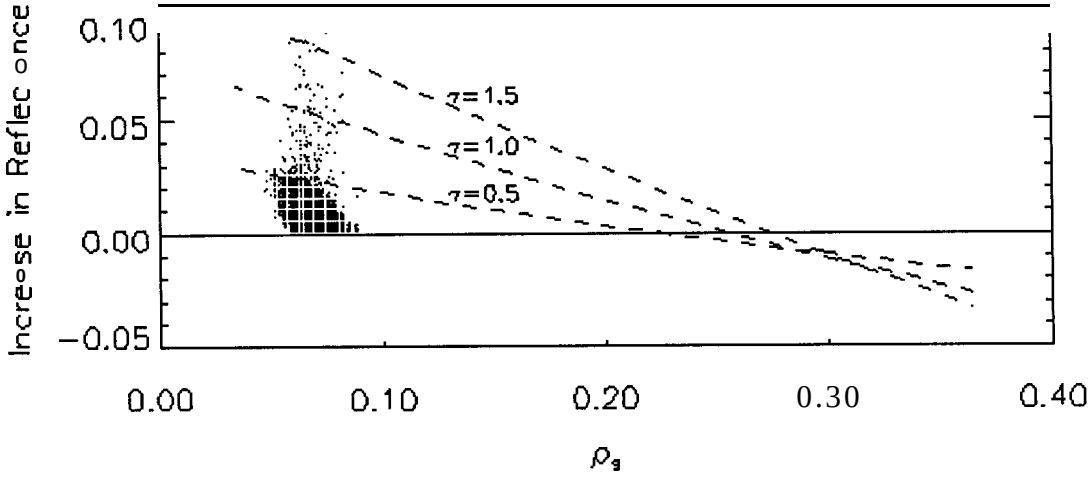

Figure 2 -An example of the critical albedo near ρ_s = 0.3. Dashed lines are changes in reflectance as calculated by the A/D model due to differing optical depths. Points are actual pixels from a GOES-8 image over Shenandoah N.P.

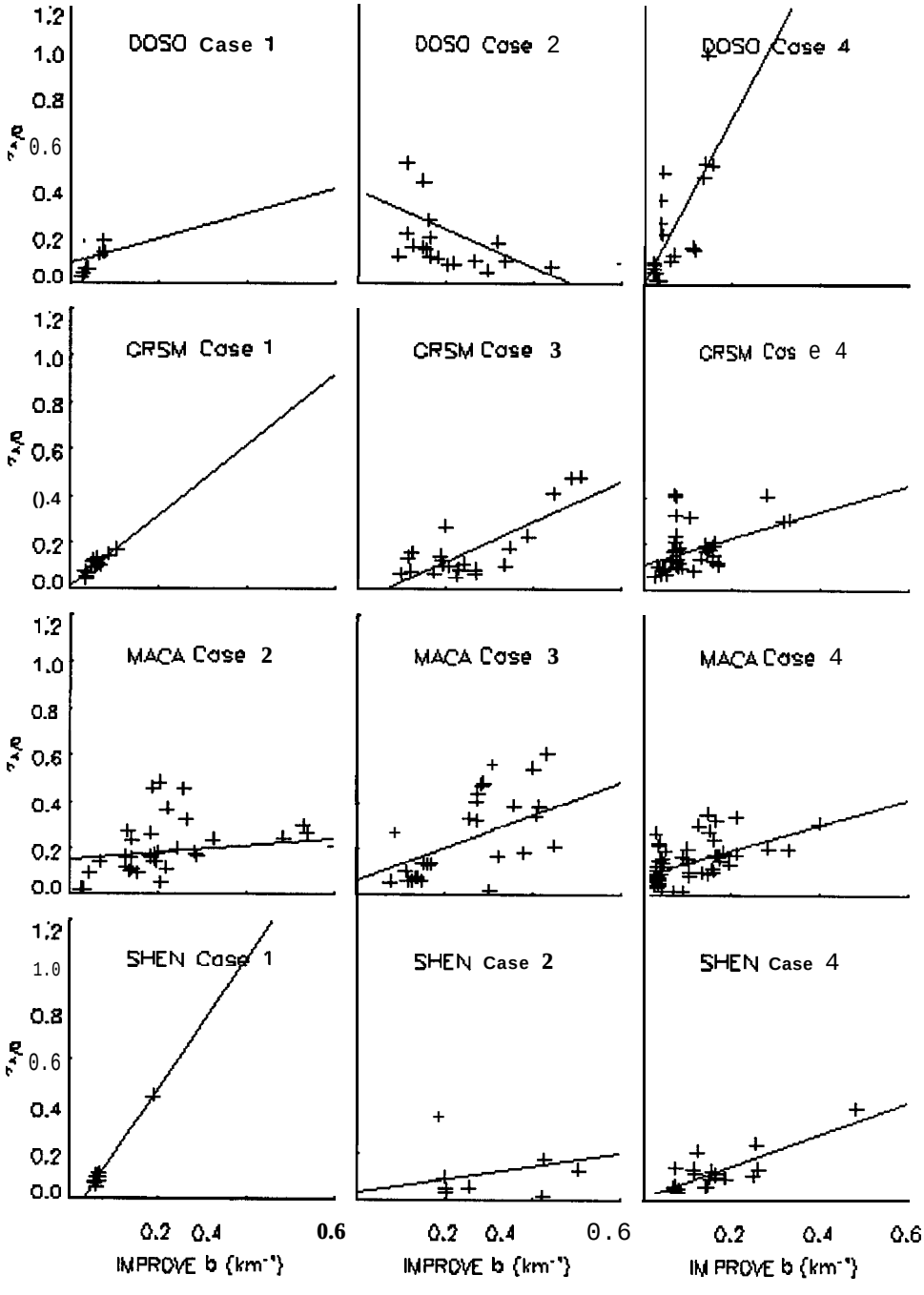

Figure 3 - Scatter plots of retrieved optical depths ($\tau_{A/D}$) vs. coefficients measured by the IMPROVE network. Lines represent linear regression best fit.

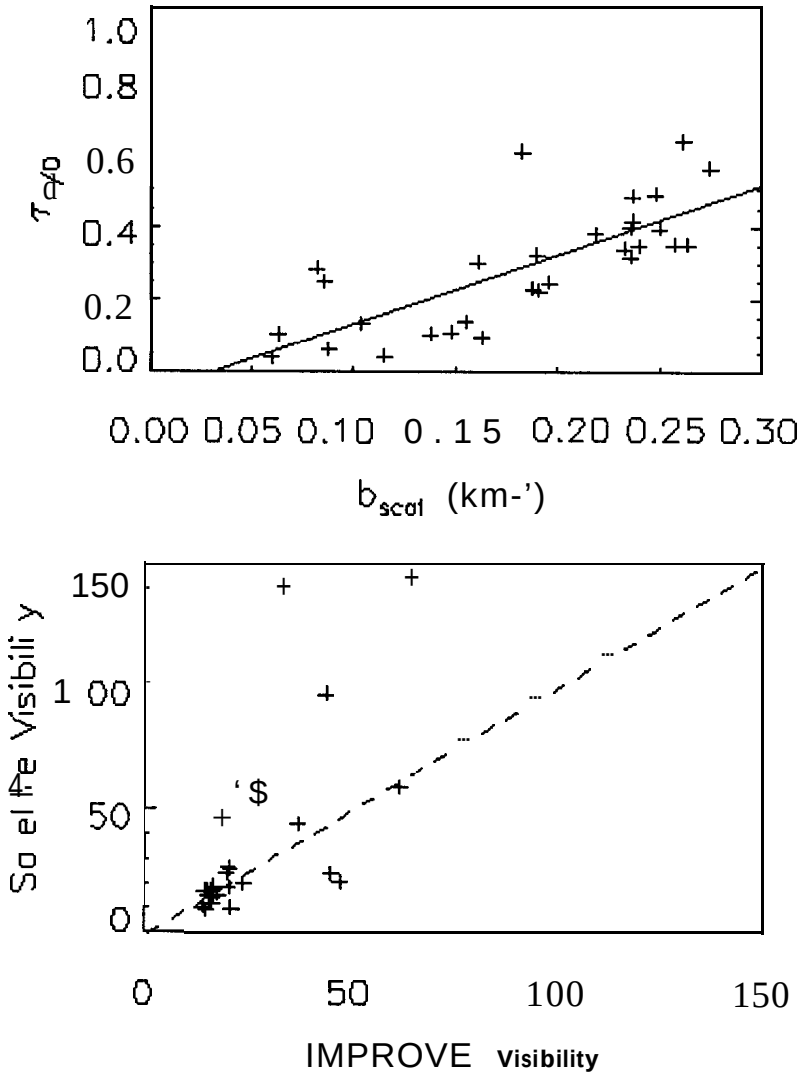

Figure 4 - a) Scatter plot of GRSM case 2 (not shown in fig. 3). Line represents linear regression best fit. b) Scatter plot of GRSM case 2 converted to visibility using $\Delta z = 1.5$ km. Dashed line is the one-to-one line.